

## Determination of the Magnitude and Sign of the ${}^2J_{\text{Pt-P}}$ Coupling Constants in Dinuclear Platinum(I) Phosphine Complexes by Two-Dimensional ${}^{31}\text{P}$ NMR Spectroscopy

Jane V. Zeile Krevor,\* Ursula Simonis, Annette Karson, Claire Castro, and Mohammed Aliakbar

Received January 30, 1991

Two-dimensional  ${}^{31}\text{P}$  homonuclear shift correlated spectroscopy (COSY) is applied to the analysis of a series of dinuclear Pt(I) complexes containing phosphine ligands. On the basis of the spectra of known symmetrical dimers, it is established that cross-peak positions of the Pt-P satellite signals can be used to determine the sign and magnitude of the  ${}^2J_{\text{Pt-P}}$  coupling constant. This coupling constant has been correlated with the strength of the Pt-Pt interaction in these complexes. Using cross-peak positions present in the spectra of unsymmetrical dimers which contain five or more phosphorus nuclei, previously unobtainable values for the  ${}^2J_{\text{Pt-P}}$  coupling constants are determined. The signs and the magnitudes of these coupling constants are found to follow the trans effect trend established for ligands in other Pt complexes.

### Introduction

During the investigation of the electrochemistry of the Pt(I) dinuclear complex  $\text{Pt}_2\text{Cl}_2(\text{dppm})_2$  (**1**) (where dppm = bis(diphenylphosphino)methane), we utilized  ${}^1\text{H}$  and  ${}^{31}\text{P}$  NMR spectroscopy for the identification of intermediates and reaction products.<sup>1</sup> Due to the complexity of some of the one-dimensional  ${}^{31}\text{P}$  NMR spectra as a result of second-order effects and the 38% abundance of  ${}^{195}\text{Pt}$  ( $I = 1/2$ ), we became interested in the application of two-dimensional  ${}^{31}\text{P}$  homonuclear shift correlated spectroscopy (COSY) to the analysis of Pt(I) dinuclear complexes containing four or more phosphorus nuclei. There have been only a few reports in the literature in which two-dimensional  ${}^{31}\text{P}$  COSY experiments have been utilized for the structural determination of phosphorus-containing compounds; most of these involve molecules of biological interest.<sup>2</sup> In two other papers the  ${}^{31}\text{P}$  COSY experiment was used to analyze the structure of a dinuclear Ru-Co complex<sup>3</sup> and to determine the sign of the  ${}^2J_{\text{P-P}}$  coupling constants for some tungsten complexes containing phosphine ligands.<sup>4</sup> Even though it has been established that two-dimensional chemical shift correlation spectroscopy is useful for the definitive assignment of coupled nuclei in complex molecules,<sup>5</sup> there has been only one very recent report of the use of this technique for the analysis of platinum clusters containing phosphine ligands.<sup>6</sup> This may be in part due to the satisfactory results provided by numerous one-dimensional  ${}^1\text{H}$  and  ${}^{31}\text{P}$  NMR studies performed on Pt(I) and Pt(II) phosphine complexes.<sup>7</sup> For complexes with simple spin systems, the one-dimensional spectra provide all information necessary (i.e. the magnitudes and signs of the  ${}^1J_{\text{Pt-P}}$  and  ${}^2J_{\text{Pt-P}}$  coupling constants) to obtain valuable structural information on these systems. However, as the spin system becomes more complex, complete analysis of the spectra may become limited by poorly resolved or overlapping resonances. An example of this limitation is found in the analysis of the  ${}^{31}\text{P}$

NMR spectra of several Pt(I) dimers from which the two-bond Pt-P ( ${}^2J_{\text{Pt-P}}$ ) coupling constants could not be determined.<sup>8</sup> These coupling constants provide important information about the nature of the Pt-Pt and Pt-ligand bonding present in these types of dimers.<sup>9-11</sup> From our own studies on a variety of Pt(I) and Pt(II) phosphine complexes, we have found that the COSY experiment yields very useful structural information which we will discuss in detail in a following paper.<sup>12</sup> In addition, the observed cross correlations not only can be used to determine the one-bond Pt-P ( ${}^1J_{\text{Pt-P}}$ ) coupling constant but also can be used for the determination of the two-bond Pt-P coupling constants even when the resonances due to Pt-P coupling are not well resolved. This will be discussed below. It is known that the heterocouplings  $J_{\text{P-H}}$  and  $J_{\text{P-C}}$  can be measured from COSY spectra in examples where the one-dimensional spectra appear complex.<sup>13</sup> In addition, it has been shown that the off-diagonal peaks in the  ${}^{13}\text{C}$  COSY spectra for a series of ruthenium carbonyl complexes are an indication of the relative signs of the  ${}^2J_{\text{P-C}}$  coupling constants.<sup>14</sup>

Complexes like **1** shown in Figure 1 with its structure and spin system represent an important class of platinum compounds in which two platinum metal centers are held adjacent by bridging phosphine ligands.<sup>15</sup> Many other platinum dimers having a structure similar to that of **1** have been synthesized and characterized.<sup>16</sup> Among these compounds, there is a wide variation in the Pt-Pt interaction, ranging from the presence of a Pt-Pt bond in some complexes to no Pt-Pt bond in others.

The spin systems of these dimers are complex and have been analyzed according to the  $X_nAA'X'_n$  nuclear magnetic system.<sup>17,18</sup> For spin system I, no  ${}^{195}\text{Pt}$  ( $I = 1/2$ ) is present; in spin system II, one  ${}^{195}\text{Pt}$  is present; and spin system III has two  ${}^{195}\text{Pt}$  nuclei. If the dimer is symmetrical, as in the case of **1**, the internal multiplet structures in the one-dimensional  ${}^{31}\text{P}$  NMR spectra are usually well resolved and the various resonances of the satellite peaks due to platinum-phosphorus coupling can be observed.<sup>15</sup> From an analysis of these satellite peaks, all the P-P and Pt-P coupling constants can be determined. Although two pathways contribute

(1) Krevor, J. V. Z.; Yee, L. *Inorg. Chem.* 1990, 29, 4305.

(2) (a) Hutton, W. C. In *Phosphorus-31 NMR, Principles and Applications*; Gorenstein, D. G., Ed.; Academic Press: Orlando, FL, 1984. (b) Bolton, P. H. In *Biomolecular Stereodynamics*; Sarma, R. H., Ed.; Adenine Press: New York, 1981; Vol. 2, p 437.

(3) Guesmi, S.; Taylor, N. J.; Dixneuf, P. H.; Carty, A. J. *Organometallics* 1986, 5, 1964.

(4) Fontaine, X. L. R.; Kennedy, J. D.; Shaw, B. L.; Vila, J. M. *J. Chem. Soc., Dalton Trans.* 1987, 2401.

(5) (a) Bax, A. *Bull. Magn. Reson.* 1985, 7, 167. (b) Morris, G. A. *Magn. Reson. Chem.* 1986, 24, 371. (c) Mann, B. E. *Adv. Organomet. Chem.* 1988, 28, 397.

(6) Kanters, R. P. F.; Schlebos, P. P. J.; Bour, J.; Steggerda, J. J.; Maas, W. E. J. R.; Janssen, R. *Inorg. Chem.* 1991, 30, 1709.

(7) (a) Appleton, T. G.; Bennett, M. A.; Tomkins, I. B. *J. Chem. Soc., Dalton Trans.* 1976, 439. (b) Sanger, A. R. *J. Chem. Soc., Dalton Trans.* 1977, 1971. (c) Slack, D. A.; Baird, M. C. *Inorg. Chim. Acta* 1977, 24, 277. (d) Hietkamp, S.; Stuffken, D. J.; Vrieze, K. *J. Organomet. Chem.* 1979, 169, 107. (e) Pryde, A.; Shaw, B. L.; Weeks, B. *J. Chem. Soc., Dalton Trans.* 1976, 322. (f) Goodfellow, R. J.; Taylor, B. R. *J. Chem. Soc., Dalton Trans.* 1974, 1676. (g) Hassan, F. S. M.; McEwan, D. M.; Pringle, P. G.; Shaw, B. L. *J. Chem. Soc., Dalton Trans.* 1985, 1501.

(8) Brown, M. P.; Franklin, S. J.; Puddephatt, R. J.; Thomas, M. A.; Seddon, K. R. *J. Organomet. Chem.* 1979, 178, 281.

(9) Koie, Y.; Shinoda, S.; Saito, Y. *Inorg. Chem.* 1981, 20, 4408.

(10) Brown, M. P.; Fisher, J. R.; Franklin, S. J.; Puddephatt, R. J.; Seddon, K. R. *J. Organomet. Chem.* 1978, 161, C46.

(11) Blau, R. J.; Espenson, J. H. *Inorg. Chem.* 1986, 25, 878.

(12) Krevor, J. V. Z.; Simonis, U.; Karson, A. Manuscript in preparation.

(13) McFarlane, W. In *Phosphorus-31 NMR Spectroscopy in Stereochemical Analysis*; Verkade, J. G., Quin, L. D., Eds.; VCH: Deerfield Beach, FL, 1987; p 145.

(14) Randall, L. H.; Cherkas, A. A.; Carty, A. J. *Organometallics* 1989, 8, 568.

(15) Brown, M. P.; Puddephatt, R. J.; Rashidi, M.; Seddon, K. R. *J. Chem. Soc., Dalton Trans.* 1977, 951.

(16) Brown, M. P.; Fisher, J. R.; Puddephatt, R. J.; Seddon, K. R. *Inorg. Chem.* 1979, 18, 2808.

(17) Pople, J. A.; Schneider, W. G.; Bernstein, H. J. *Can. J. Chem.* 1957, 35, 1060.

(18) (a) Harris, R. K. *Can. J. Chem.* 1964, 42, 2275. (b) Sheppard, W.; Turner, J. J. *Proc. R. Soc. London* 1959, 252, 506.

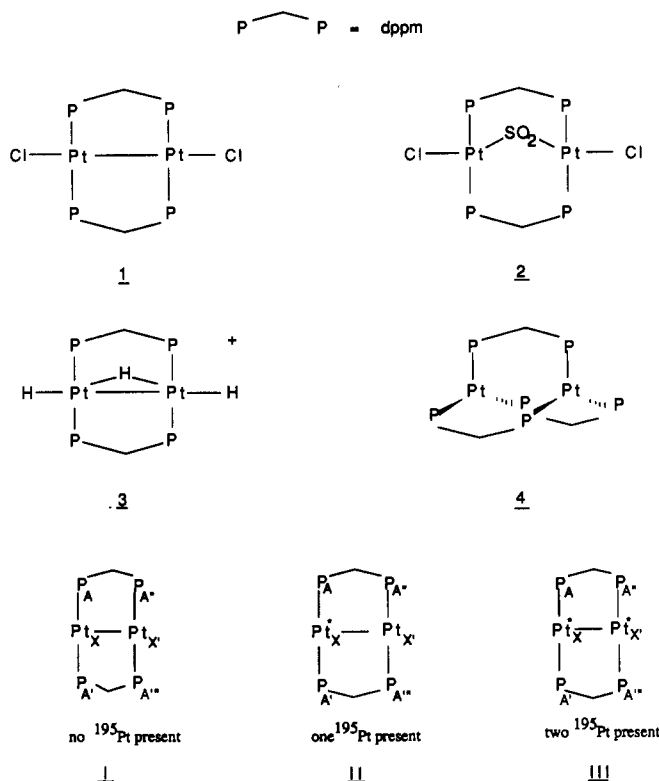


Figure 1. Structures of complexes 1–4 and their nuclear magnetic spin systems.

to the  $^2J_{Pt-P}$  coupling constant, it is usually calculated from the equation  $N' = ^1J_{Pt-P} + ^2J_{Pt-P}$ , where  $N'$  is the measured separation between the resonances of a doublet that results from the presence of two magnetically active  $^{195}Pt$  nuclei as shown in structure III, Figure 1.<sup>10,15</sup> This measurement is dependent upon the presence of well-resolved Pt–P couplings, as is observed for 1. In the case of unsymmetrical dimers, particularly when one of the chloride ligands of 1 has been replaced by another phosphine ligand, the coupling pattern in the  $^{31}P$  NMR spectra is more complex and the satellite peaks are not well resolved because of long-range P–P couplings.<sup>8,19</sup> Hence, the determination of the  $^2J_{Pt-P}$  coupling constants either has not been possible or has required spectral simulation to verify calculated possibilities.

The importance of the  $^2J_{Pt-P}$  coupling constants in these dinuclear platinum(I) phosphine complexes is found in the correlation of its magnitude and sign to the nature of the Pt–Pt interaction present. For structure II, Figure 1, the  $^2J_{Pt-P}$  coupling constant will have two contributing pathways.<sup>10</sup> One is a two-bond pathway through the Pt–Pt bond,  $^2J_{Pt-P_A''}$  (where the asterisk represents a  $^{195}Pt$  nucleus, Figure 1), and the other is a three-bond pathway through the methylene group of the dppm ligand,  $^3J_{Pt-P_A''}$ . It has been shown that the  $^2J_{Pt-P_A''}$  coupling constant is negative and the  $^3J_{Pt-P_A''}$  coupling constant is positive. Hence, the magnitude and sign of the measured  $^2J_{Pt-P}$  coupling constant are an indication of the presence of a Pt–Pt bond and a measure of the relative length of that bond.<sup>10</sup> From one-dimensional NMR studies, it has been determined that a large, negative value for  $^2J_{Pt-P}$  results when a strong Pt–Pt bond is present.<sup>11</sup> As the Pt–Pt bond weakens, the  $^2J_{Pt-P}$  coupling constant becomes more positive. This is a result of the  $^3J_{Pt-P_A''}$  coupling pathway becoming more significant relative to the  $^2J_{Pt-P_A''}$  pathway. In the absence of a Pt–Pt bond, the  $^3J_{Pt-P_A''}$  coupling is most important and will result in a large, positive value for  $^2J_{Pt-P}$ .<sup>10</sup>

We now report the results of our investigation of the application of the  $^{31}P$  COSY experiment to Pt(I) dimers containing phosphine ligands taking advantage of the chemical shift dispersion over two

spectral dimensions.<sup>20</sup> We will show not only that cross-peak information can be used to determine the presence of coupling between two phosphorus nuclei but also that the magnitude and sign of the  $^2J_{Pt-P}$  coupling constant can be determined directly from the two-dimensional spectra by means of the relative positions of the satellite cross peaks with respect to the main phosphorus resonance. This coupling constant can be determined even in cases where clearly resolved platinum satellite peaks are not obtained.

**Experimental Section**

**Preparation of Compounds.** All platinum compounds were synthesized according to published procedures.<sup>1,8,15,16,19,27,28</sup> Bis(diphenylphosphino)methane (Strem) and triphenylphosphine (Aldrich) were used as received. SO<sub>2</sub> gas was generated from the mixture of concentrated HCl (EM Science) and sodium sulfite (Spectrum). Nondeuterated solvents (EM Science) were dried and distilled under N<sub>2</sub> prior to use. Deuterated solvents (Aldrich) were used as received.

**NMR Spectroscopy.** One-dimensional proton NMR spectra taken at room temperature were recorded on a General Electric QE 300-MHz NMR spectrometer equipped with a 1280 computer system, locked on solvent deuterium, and referenced to tetramethylsilane (TMS) used as an internal standard. Solvents most frequently used were CDCl<sub>3</sub> and CD<sub>2</sub>Cl<sub>2</sub>, and the concentrations of the samples were about 2.0 mM. Typically, one-dimensional <sup>1</sup>H spectra of the Pt(I) dinuclear phosphine complexes were acquired by using spectral widths of 6024 Hz, 16K data points, and 1-s repetition time. In general, 32 transients were obtained with a 3-μs pulse (90° pulse = 9 μs).

The one-dimensional <sup>31</sup>P NMR spectra of these complexes were taken at room temperature on a General Electric GN 300-MHz NMR spectrometer equipped with a 1280 computer system and a process controller using a 10-mm multinuclear probe. Typically, the data were acquired by using spectral widths of 20 000 Hz, 16K data points, a recycle delay of 5 s, and broad-band proton decoupling. In general, 256 transients were obtained with an 18-μs 90° pulse. A solution of trimethyl phosphate (TMP) in deuteriobenzene served as an external reference.

Two-dimensional <sup>31</sup>P homonuclear shift correlation (COSY) spectra of complexes 2–9, were recorded on the General Electric GN 300-MHz instrument. Quadrature detection was used with typically a sweep width of 6024 Hz in F<sub>2</sub> and ±3012 Hz in F<sub>1</sub>. The size in F<sub>2</sub> was 1024 w (words). A total of 256 FIDs were taken in F<sub>1</sub>, with 256 scans each. The recycle delay was set to 1 s to give a total measuring time of about 18 h. A nonshifted sine bell was used to process the two-dimensional data set. The data were zero-filled in F<sub>1</sub> to give a final matrix of 512 w × 512 w. No proton decoupling was applied.

The <sup>31</sup>P COSY experiment for complex 1 was performed on a General Electric GN 500-MHz NMR spectrometer equipped with a 1280 computer system and a process controller at GE Instruments in Fremont, CA. Data were acquired and processed as described above with the exception that the FIDs were apodized by double-exponential multiplication.

**Results and Discussion**

In order to demonstrate the successful application of the COSY experiment to the Pt(I) dimers, two groups of previously characterized dimers were chosen. One exhibits simple, well-resolved <sup>31</sup>P NMR spectra, and the other has more complex spectra. The first group of dimers discussed includes the four symmetrical complexes 1–4, shown in Figure 1, in which the sign and magnitude of the  $^2J_{Pt-P}$  coupling have been previously determined from the analysis of well-resolved platinum satellite peaks present in the one-dimensional spectra. The second group consists of unsymmetrical dimers in which either the  $^2J_{Pt-P}$  coupling constant or its sign has not been previously reported.

(19) Blau, R. J.; Espenson, J. H.; Kim, S.; Jacobson, R. A. *Inorg. Chem.* 1986, 25, 757.

(20) This publication is taken in part from the M.S. thesis of A.K.  
 (21) Grossel, M. C.; Brown, M. P.; Nelson, C. D.; Yavari, A.; Kallas, E.; Moulding, R. P.; Seddon, K. R. *J. Organomet. Chem.* 1982, 232, C13.  
 (22) Titman, J. J.; Keeler, J. J. *Magn. Reson.* 1990, 89, 640.  
 (23) McFarlane, W. J. *Chem. Soc. A.* 1967, 1922.  
 (24) Drago, R. S. *Physical Methods in Chemistry*; W. B. Saunders: Philadelphia, PA, 1977; p 280.  
 (25) von Philipsborn, W. *Angew. Chem., Int. Ed. Engl.* 1971, 10, 472.  
 (26) Muralidharan, S.; Espenson, J. H.; Ross, S. A. *Inorg. Chem.* 1986, 25, 2557.  
 (27) Brown, M. P.; Puddephatt, R. J.; Rashidi, M.; Seddon, K. R. *J. Chem. Soc., Dalton Trans.* 1978, 516.  
 (28) Brown, M. P.; Fisher, J. R.; Hill, R. H.; Puddephatt, R. J.; Seddon, K. R. *Inorg. Chem.* 1981, 20, 3516.

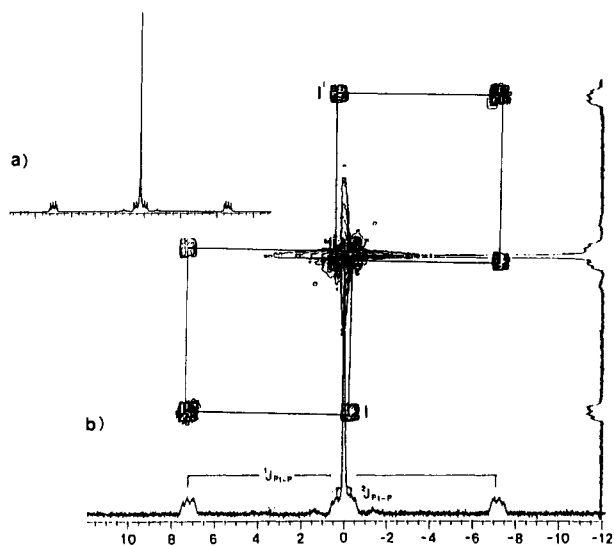


**Figure 2.** (a) One-dimensional proton-decoupled  $^{31}\text{P}$  NMR spectrum of  $\text{Pt}_2\text{Cl}_2(\text{dppm})_2$  (1) and (b) one- and two-dimensional  $^{31}\text{P}$  NMR spectra of 1. Boxes indicate the  $P_A$ ,  $P_{A'}$ ,  $P_{A''}$ , and  $P_{A'''}$  couplings due to structures II and III, Figure 1.

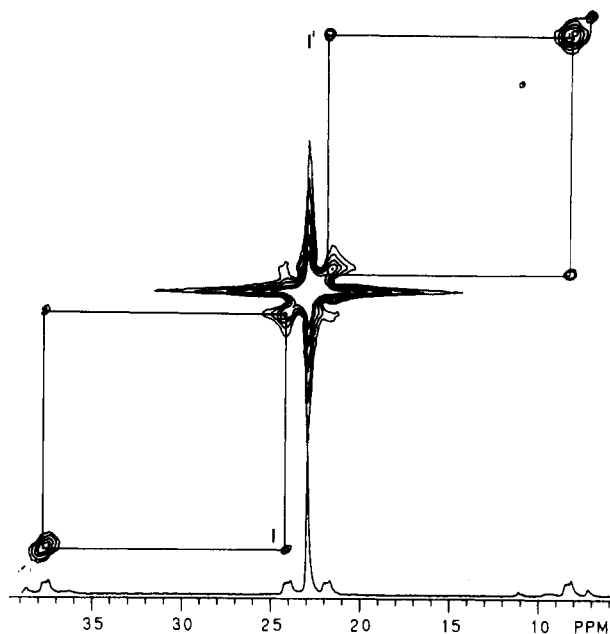
The structures of the four symmetrical dimers, 1–4, shown in Figure 1 and studied by two-dimensional NMR spectroscopy, have a similar  $\text{Pt}_2(\text{dppm})_2$  unit, which will result in three possible spin systems, I–III, Figure 1.<sup>15</sup> Note that although 3 is not planar, the symmetrical nature of its structure does result in the same three spin possibilities so that its  $^{31}\text{P}$  NMR spectrum can be analyzed in the same way.<sup>21</sup>

Figure 2a shows the one-dimensional, proton-decoupled  $^{31}\text{P}$  NMR spectrum of 1. In this spectrum, one large resonance centered at 6.77 ppm is observed for the four equivalent phosphorus atoms present in structure I, and in addition, two sets of satellite peaks are observed due to the presence of  $^{195}\text{Pt}$ .<sup>15</sup> One set of satellite peaks is centered around the main phosphorus resonance but is well separated from it, exhibiting a large coupling constant. It results from the  $^1J_{\text{Pt-P}}$  coupling that is present due to structures II and III. From here on, we will refer to them as outer satellite peaks. The other set of satellite peaks, the inner set, at the base of the main phosphorus resonance is a result of the much smaller  $^2J_{\text{Pt-P}}$  coupling that is present. A thorough analysis of this spectrum has been done in which the  $^2J_{\text{Pt-P}}$  coupling constant was experimentally determined from  $N'$ , where  $N' = ^1J_{\text{Pt-P}} + ^2J_{\text{Pt-P}}$ .<sup>5,15</sup>

Figure 2b shows the proton-coupled two-dimensional  $^{31}\text{P}$  NMR spectrum of 1, including the one-dimensional proton-phosphorus-coupled spectrum. As a result of the P–H couplings, this one-dimensional spectrum does not show the well-resolved platinum satellite peaks as observed in Figure 2a. In the two-dimensional spectrum, the diagonal peaks due to the inner set of satellite peaks are obscured by the central phosphorus resonance. However, of main interest are the cross correlations that are observed in the two-dimensional spectrum shown in Figure 2. As depicted in the figure, cross peaks are observed between the outer and inner set of satellite peaks. These cross peaks are due to P–P coupling and clearly show the known pattern by which the four phosphorus nuclei,  $P_A$ ,  $P_{A'}$ ,  $P_{A''}$ , and  $P_{A'''}$ , are coupled to each other.<sup>15</sup> The cross peaks, marked I and I', are of specific interest because their distance to each other represents the  $^2J_{\text{Pt-P}}$  coupling in 1. The off-diagonal peak, I, is slightly upfield from the main phosphorus resonance whereas the corresponding off-diagonal peak, I', is slightly downfield from the main phosphorus resonance. The horizontal separation between the centers of these two cross peaks is equivalent to the magnitude of the  $^2J_{\text{Pt-P}}$  coupling constant.<sup>22</sup> Values of  $^2J_{\text{Pt-P}}$  coupling constants determined in this way for these complexes are consistent with previously known values as shown in Table I. This method of determining the magnitude of  $^2J_{\text{Pt-P}}$  from the COSY spectrum has two important advantages over the one determined from the one-dimensional spectrum: (1)

**Table I.**  $^{31}\text{P}$  NMR Data from the 1D and 2D  $^{31}\text{P}$  NMR Spectra

complex	$\delta(P_A)$ , ppm <sup>a</sup>	coupling consts, Hz (this paper; lit. (ref))	
		$^1J_{\text{Pt-P}}$	$^2J_{\text{Pt-P}}$
$\text{Pt}_2\text{Cl}_2(\text{dppm})_2$ (1)	-0.11	2722; 2936 (15)	-123; -134 (15)
$\text{Pt}_2\text{Cl}_2\text{SO}_2(\text{dppm})_2$ (2)	22.94	3566; 3588 (16)	+272; +273 (16)
$[\text{Pt}_2\text{H}_3(\text{dppm})_2]\text{Cl}$ 3	20.03	2778; 2769 (27)	+36; +16.6 (27)
$\text{Pt}_2(\text{dppm})_3$ (4)	42.14	4451; 4456 (21)	+52; +51 (21)



**Figure 3.** One- and two-dimensional  $^{31}\text{P}$  NMR spectra of  $\text{Pt}_2\text{Cl}_2\text{SO}_2(\text{dppm})_2$  (2). Boxes indicate the  $P_A$ ,  $P_{A'}$ ,  $P_{A''}$ , and  $P_{A'''}$  coupling due to structures II and III, Figure 1.

the determination can be made directly from the experimental data and is not calculated from two other measurements, as in the previous method which relies on the  $N'$  equation, and (2) it can be made even if the satellite peaks in the one-dimensional spectrum are not well resolved or are obscured by the main phosphorus resonances.

In addition to directly measuring the magnitude of  $^2J_{\text{Pt-P}}$ , it is also possible to determine the sign of this coupling constant from the COSY spectrum. Since the sign of the  $^1J_{\text{Pt-P}}$  coupling constant is always positive,<sup>23</sup> the coupling between the inner satellite peaks and the outer satellite peaks will depend upon the sign of the  $^2J_{\text{Pt-P}}$  coupling constant.<sup>24</sup> In other words, if the sign of  $^2J_{\text{Pt-P}}$  is negative, coupling will be observed between a low-field satellite peak and a high-field satellite peak. This will be indicated by cross peak I appearing upfield from the main phosphorus resonance and the corresponding cross peak I' appearing downfield from it. This is observed in Figure 2b. If  $^2J_{\text{Pt-P}}$  is positive, the two low-field satellite peaks (on the left side of the central phosphorus resonance) will be coupled to each other and the two high-field satellite peaks (on the right side of the central phosphorus resonance) will be coupled to each other. This is observed in Figure 3, as discussed below. From one-dimensional spectra it is not possible to determine the relative coupling between satellite peaks unless other experiments using selective homonuclear decoupling or spin ticking are done.<sup>25</sup> These experiments can be time consuming and usually require well-resolved resonances. In the COSY experiment however, the relative position of the inner satellite peaks will be indicated by the positions of the cross peaks relative to the main phosphorus resonance.

For complex 1, the sign of  $^2J_{\text{Pt-P}}$  has previously been determined to be negative.<sup>15</sup> Therefore, the position of cross peak I in Figure 2b should be slightly upfield from the main phosphorus resonance. This upfield cross peak should show a cross correlation to a downfield satellite peak. As can be seen, this is indeed the case. Thus, it can be concluded that when the cross peak which is coupled to the downfield satellite peak is to the right of the main

phosphorus resonance, the sign of  $^2J_{Pt-P}$  will be negative. Further examples which support this conclusion will be shown using more complex spectra later in this paper.

As described above, if the sign of  $^2J_{Pt-P}$  is positive, the high field inner satellite peak should be coupled to the high-field outer satellite peak and the downfield inner satellite peak should be coupled to the downfield outer satellite peak. This will be indicated in the two-dimensional spectrum by the position of the cross peak correlated to the low-field outer satellite peak being to the left (low-field side) of the main phosphorus resonance. This is observed to be true in Figure 3, which shows the two-dimensional <sup>31</sup>P NMR spectrum of complex 2. The cross peak depicted as I appears to the left of the main phosphorus resonance, and the cross peak depicted as I' appears to the right of this resonance. It has been reported that the  $^2J_{Pt-P}$  coupling for this complex has a positive sign and a value of 273 Hz.<sup>12,26</sup> It can clearly be seen in Figure 3 that the inner set of satellite peaks are well separated from the main central phosphorus resonance, which is consistent with a larger coupling constant. In the two-dimensional spectrum, the position of cross peak I clearly shows that the sign of the  $^2J_{Pt-P}$  coupling constant for 2 is positive. The horizontal separation of the centers of peaks I and I' measured is 272 Hz, which is consistent with the previously reported value (see Table I).

Another example in which the  $^2J_{Pt-P}$  coupling is known to be positive is complex 3.<sup>27</sup> In this case, the magnitude of this coupling is only 17 Hz, which means that the inner set of satellite peaks is not clearly separated from the main phosphorus resonance in the one-dimensional spectrum. However, as in the case of 1 and 2, the cross peaks present between the two sets of satellite peaks clearly show that the  $^2J_{Pt-P}$  coupling constant is positive. The magnitude of  $^2J_{Pt-P}$  as determined from the separation between the cross peaks correlates with the previously reported value as shown in Table I. The one- and two-dimensional spectra of 3 can be found in the supplementary material of this paper.

Complex 4 also has a positive  $^2J_{Pt-P}$  coupling.<sup>21</sup> This positive coupling is observed directly in the two-dimensional spectrum of 4, which is included in the supplementary material. The downfield inner satellite resonance is coupled to the downfield resonance of the outer satellite peaks, as shown by cross peak I being slightly downfield from the central phosphorus resonance. The measured value of the  $^2J_{Pt-P}$  coupling constant from the two-dimensional spectrum is given in Table I.

On the basis of the results of the two-dimensional NMR correlation spectroscopy of the four symmetrical complexes, 1-4, we have concluded that the COSY experiment provides an effective method for determining the magnitude and sign of the  $^2J_{Pt-P}$  coupling constant. To verify this conclusion, we have applied this technique to the unsymmetrical dimers, 5-9, which show a more complex coupling pattern in their one-dimensional spectra. These complexes differ from complexes 1-4 in that one of the chloride or hydride ligands is replaced by another phosphine (5-8) or by a carbonyl group (9).

The structures of complexes 5-9 and their resulting spin systems are shown in Figure 4. For each of these complexes, there are at least three chemically inequivalent phosphorus nuclei denoted as P<sub>A</sub>, P<sub>B</sub>, and P<sub>C</sub>. In previously published <sup>31</sup>P NMR data for complexes 6-8, the  $^2J_{Pt-P_A}$  and  $^2J_{Pt-P_B}$  coupling constants were not reported probably because of the complexity of the satellite peaks of the P<sub>A</sub> and P<sub>B</sub> resonances.<sup>28</sup> For complex 5,  $^2J_{Pt-P_A}$  and  $^2J_{Pt-P_B}$  were determined by spectral simulation but the sign could not be specified.<sup>19</sup> However, we have found that the cross peak information present in the two-dimensional spectra of all of these complexes can be used to yield the  $^2J_{Pt-P_A}$  and  $^2J_{Pt-P_B}$  coupling constants directly.

Figure 5 shows the one- and two-dimensional <sup>31</sup>P NMR spectra of complex 5. As can be seen, the spectrum is more complex because there are three chemically inequivalent phosphorus nuclei, P<sub>A</sub>, P<sub>B</sub>, and P<sub>C</sub>, each with their own set of platinum satellite peaks. Because of the multiple coupling pathways possible between these three phosphorus nuclei, more cross peaks are observed in the two-dimensional spectrum of 5 than in the two-dimensional spectra of 1-4. Analysis of the cross correlations reveal that P<sub>A</sub> is coupled

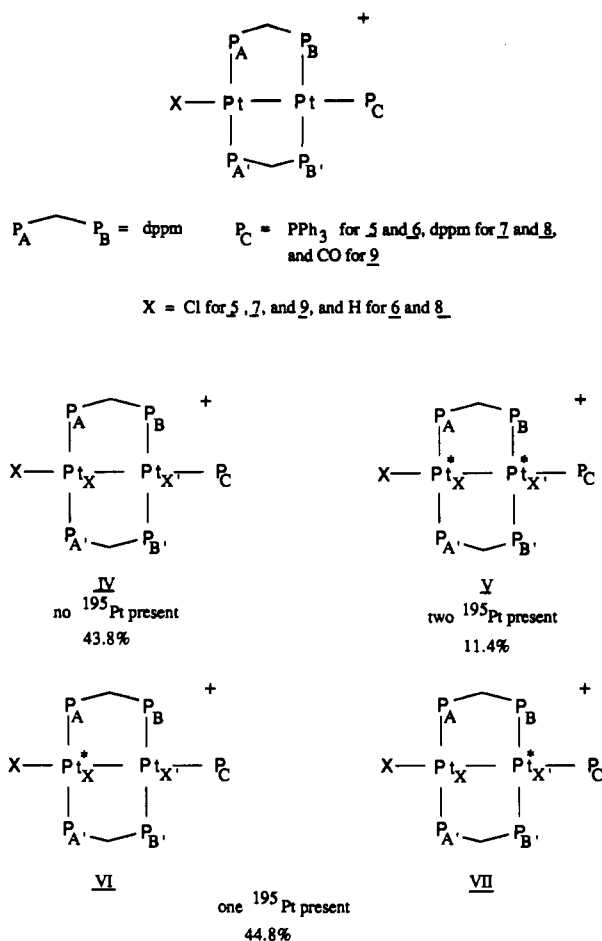


Figure 4. Structures of complexes 5-9 and their nuclear magnetic spin systems.

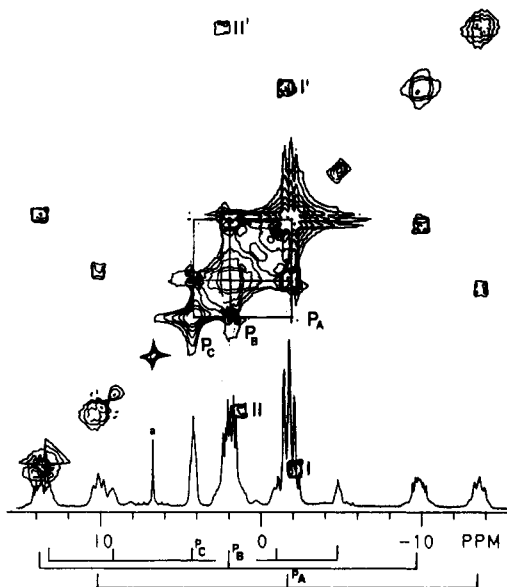


Figure 5. One- and two-dimensional <sup>31</sup>P NMR spectra of [Pt<sub>2</sub>Cl(dppm)<sub>2</sub>PPh<sub>3</sub>]Cl (5). The scalar coupling between P<sub>A</sub>, P<sub>B</sub>, and P<sub>C</sub> is shown by the boxes. The resonance marked a is due to Pt<sub>2</sub>Cl<sub>2</sub>(dppm)<sub>2</sub>.

to P<sub>B</sub>, P<sub>B</sub> is coupled to both P<sub>A</sub> and P<sub>C</sub>, and P<sub>C</sub> is coupled to P<sub>B</sub>. This coupling is indicated in Figure 5 by the boxes drawn connecting the main resonance on the diagonal with the corresponding off-diagonal peaks. In addition, it can be seen that P<sub>A</sub> is coupled to P<sub>C</sub>. This three-bond coupling is weaker than the two-bond coupling present between P<sub>B</sub> and P<sub>C</sub>, which is indicated by the smaller size of the cross peak present between P<sub>A</sub> and P<sub>C</sub>.<sup>29</sup>

**Table II.** Chemical Shifts and Coupling Constants from the 1D and 2D  $^{31}\text{P}$  NMR Spectra

complex	$\delta(\text{P}_A, \text{P}_B, \text{P}_C)$ , ppm <sup>a</sup>	coupling consts, Hz (first row, this paper; second row, lit. (ref))					
		$^1J_{\text{Pt-P}_A}$	$^1J_{\text{Pt-P}_B}$	$^1J_{\text{Pt-P}_C}$	$^2J_{\text{Pt-P}_C}$	$^2J_{\text{Pt-P}_A}$	$^2J_{\text{Pt-P}_B}$
[Pt <sub>2</sub> Cl(dppm) <sub>2</sub> PPh <sub>3</sub> ]Cl (5)	-1.8, 1.9, 4.2	2886	2856	2207	1229	-84	-137
		2894 (19)	2876 (19)	2186 (19)	1232 (19)	±37 (18)	±142 (19)
[Pt <sub>2</sub> Cl(dppm) <sub>3</sub> ]Cl (7)	-1.8, 1.3, -1.8 <sup>b</sup>	2844	2913	2071	1242	-76 (d)	-119 (d)
		2872 (19, 1)	2921 (19, 1)	2146 (19, 1)	1270 (19, 1)		
[Pt <sub>2</sub> H(dppm) <sub>2</sub> PPh <sub>3</sub> ]Cl (6)	11.6, 12.0, 31.0	3508	2897	2192	583	-99 (d)	-54 (d)
		3532 (28)	2894 (28)	2181 (28)	596 (28)		
[Pt <sub>2</sub> H(dppm) <sub>3</sub> ]Cl (8)	10.7, 11.6, 26.4 <sup>c</sup>	3533	2874	2720	1364	-85 (d)	-12 (d)
		3540 (28)	2880 (28)	2134 (28)	620 (28)		
[Pt <sub>2</sub> CO(dppm) <sub>2</sub> Cl]Cl (9)	-9.06, -7.94	2714	2581	<sup>e</sup>	<sup>e</sup>	-45	-58 (d)
		2711 (8)	2591 (8)			±62 (10)	

<sup>a</sup>Relative to TMP. <sup>b</sup>P<sub>D</sub> at -26.9. <sup>c</sup>P<sub>D</sub> at -28.0. <sup>d</sup>Not reported. <sup>e</sup>Not applicable.

The remaining two sets of cross peaks present in Figure 5 are marked I, I' and II, II'. These cross peaks are due to the presence of the inner set of satellite peaks for the P<sub>A</sub> and P<sub>B</sub> resonances that arise from the long-range  $^2J_{\text{Pt-P}}$  coupling expected for structures VI and VII in Figure 4. In the one-dimensional spectrum, these inner sets of satellite peaks are obscured by the main resonances for P<sub>A</sub> and P<sub>B</sub> and cannot be used to determine the values of  $^2J_{\text{Pt-P}_A}$  or  $^2J_{\text{Pt-P}_B}$ . However, by measuring the horizontal distance between the cross peaks marked I and I' and the ones marked II and II', we can determine the magnitude of these two coupling constants. These values are reported in Table II and are similar to those determined previously by spectral simulation. In addition, the relative position of the lower cross peaks, depicted as I and II, with respect to the main phosphorus resonance indicates that the signs of both coupling constants are negative. As in complex 1, the lower cross peak appears upfield from the main phosphorus resonance whereas the corresponding upper cross peak appears downfield from this resonance. The negative sign suggests that a Pt-Pt bond is present in this complex as expected.

Another example of an unsymmetrical dimer is complex 6, in which six phosphorus nuclei are present. Five of these are coordinated directly to the Pt atoms, while the sixth is at the free end of the dppm ligand which is trans to the Pt-Pt bond. Figure 6 shows the expanded regions of the one- and two-dimensional spectra of this complex. For the sake of simplicity, only the coupling patterns of P<sub>A</sub> and P<sub>B</sub> are shown. A detailed analysis of the complete spectrum will be reported in our following paper.<sup>12</sup>

Concentrating on the set of cross peaks marked I and II in Figure 6, one can see from the position of these peaks relative to their respective central phosphorus resonances that the signs of both the  $^2J_{\text{Pt-P}_A}$  and  $^2J_{\text{Pt-P}_B}$  are negative. The magnitudes of these coupling constants as determined by the separation between the cross peaks marked I and the ones marked II are reported in Table II. Neither the signs nor the magnitudes of these coupling constants have been reported previously for this complex.

In a similar manner, the two-dimensional spectra of complexes 7-9 were analyzed. The spectra for these complexes are present in the supplementary material. The magnitudes and signs of  $^2J_{\text{Pt-P}_A}$  and  $^2J_{\text{Pt-P}_B}$  were determined and are reported in Table II. In each case, the signs of the coupling constants were found to be negative. This was expected, since a Pt-Pt bond is present in each of these complexes.<sup>19,28,30</sup>

The  $^{31}\text{P}$  COSY studies clearly show that it is possible to determine the magnitude and sign of the  $^2J_{\text{Pt-P}}$  coupling constant unambiguously. We now wish to emphasize the importance of these  $^2J_{\text{Pt-P}}$  coupling constants and the value of the information they provide. A comparison of these coupling constants shows that the relative magnitude of  $^2J_{\text{Pt-P}_A}$  vs  $^2J_{\text{Pt-P}_B}$  can be predicted on the basis of the trans effect. For example, in complex 5, the ligands trans to the Pt-Pt bond are Cl<sup>-</sup> and PPh<sub>3</sub>. Because PPh<sub>3</sub>

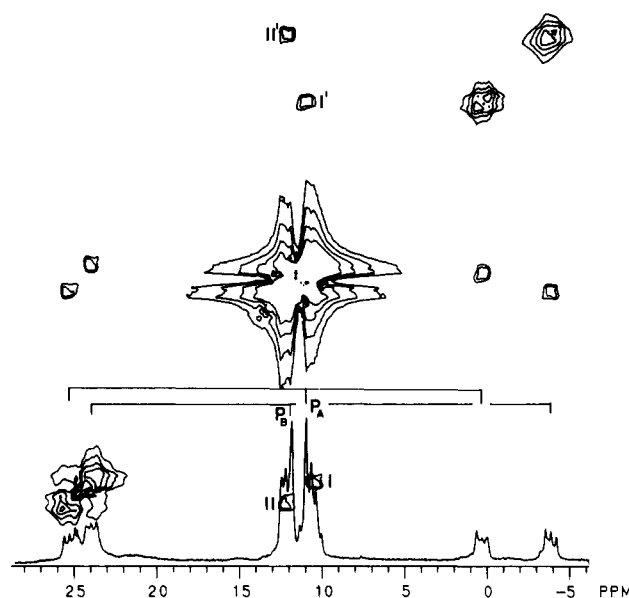


**Figure 6.** One- and two-dimensional  $^{31}\text{P}$  NMR spectra of [Pt<sub>2</sub>H(dppm)<sub>3</sub>]Cl (6). The spectrum shows only the region of the P<sub>A</sub> and P<sub>B</sub> resonances.<sup>26</sup>

exerts a greater trans influence on the Pt-Pt bond than Cl<sup>-</sup>, and  $^2J_{\text{Pt-P}_B}$  coupling constant should be larger than  $^2J_{\text{Pt-P}_A}$ . This difference would follow the trend observed by Blau and Espenson for the  $^2J_{\text{Pt-P}_C}$  coupling constants.<sup>11</sup> The values of  $^2J_{\text{Pt-P}_A}$  (-84 Hz) and  $^2J_{\text{Pt-P}_B}$  (-137 Hz) determined from the COSY spectrum support this order of trans effect.

Other examples of this trans effect order are found in complexes 8 and 9. In 8, the ligands trans to the Pt-Pt bond are H<sup>-</sup> and PPh<sub>3</sub>. Since H<sup>-</sup> has a greater trans influence on the Pt-Pt bond, the value of  $^2J_{\text{Pt-P}_A}$  should be larger than that of  $^2J_{\text{Pt-P}_B}$ . This is exactly what is observed:  $^2J_{\text{Pt-P}_A}$  is -99 Hz, and  $^2J_{\text{Pt-P}_B}$  is -54 Hz. For the ligands CO and Cl<sup>-</sup>, the trans effect has been determined to be about the same.<sup>31</sup> Therefore, in 9, the  $^2J_{\text{Pt-P}}$  values for P<sub>A</sub> and P<sub>B</sub> should be similar if not the same. From Table II, it can be seen that this is the case. For 9,  $^2J_{\text{Pt-P}_A}$  is -45 Hz and  $^2J_{\text{Pt-P}_B}$  is -58 Hz.

The trans effect is further supported by comparing the  $^2J_{\text{Pt-P}}$  values between complexes. Complexes 5 and 8 differ from each other by having either a Cl<sup>-</sup> ligand (5) or a H<sup>-</sup> ligand (8) trans to the Pt-Pt bond. In this case, the  $^2J_{\text{Pt-P}_A}$  values should be similar, but  $^2J_{\text{Pt-P}_B}$  in 5 should be larger than  $^2J_{\text{Pt-P}_B}$  in 8 because H<sup>-</sup> exerts a greater trans influence on the Pt-Pt bond than Cl<sup>-</sup>. A comparison of these  $^2J_{\text{Pt-P}}$  values shows this to be true.  $^2J_{\text{Pt-P}_A}$  for 5 is -84 Hz, and  $^2J_{\text{Pt-P}_A}$  for 8 is -99 Hz whereas  $^2J_{\text{Pt-P}_B}$  for 5 is -137 Hz and  $^2J_{\text{Pt-P}_B}$  for 8 is -54 Hz.

A similar result is obtained when the  $^2J_{\text{Pt-P}}$  values of 6 are compared with those of 7. The  $^2J_{\text{Pt-P}_A}$  values for 6 and 7 are

(29) The use of cross-peak information obtained from two-dimensional  $^{31}\text{P}$  NMR spectroscopy to determine the structural relationship between phosphine ligands in a series of Pt(I) and Pt(II) complexes is the subject of our other paper.<sup>11</sup>

(30) Manojlovic-Muir, L.J.; Muir, K. W. *J. Organomet. Chem.* 1979, 179, 479.

(31) Cotton, F. A.; Wilkinson, G. *Advanced Inorganic Chemistry*; Wiley: New York, 1980; pp 1200-1202.

similar, i.e. -85 and -76 Hz, respectively. The  $^2J_{\text{Pt-P}_B}$  coupling constant for **7** should be greater than that for **6** because of the greater trans influence of the  $\text{H}^-$  ligand in **6**. For **7**,  $^2J_{\text{Pt-P}_B}$  is -119 Hz whereas, for **6**,  $^2J_{\text{Pt-P}_B}$  is -12 Hz.

The basis for this correlation to the trans effect may be related to the difference in the electronic distribution about each platinum atom in these dimers, which is indicated by the P-Pt-P bond angles and Pt-P bond lengths.<sup>32</sup> From the crystal structure data of complexes **5**,<sup>19</sup> **8**,<sup>33</sup> and **9**,<sup>27</sup> it can be seen that, in each of these dimers, the P-Pt-P angles at  $\text{Pt}_X$  and  $\text{Pt}_X'$  are different. For example, in **5**, the  $\text{P}_A\text{-Pt}_X\text{-Pt}_A'$  angle is  $177^\circ$  whereas the  $\text{P}_B\text{-Pt}_X\text{-Pt}_B'$  angle is  $160^\circ$ . For **8** and **9**, not only are these angles different but the Pt-P bond lengths are also different. In **8**, the Pt-P<sub>A</sub> and Pt-P<sub>B</sub> bond lengths are 2.248 and 2.264 Å, respectively. Although the steric requirements of the ligands trans to the Pt-Pt bond will partially contribute to the observed structural differences, the  $\sigma$ -donor ability of these ligands, which is related to the trans effect order, will also play a role in these differences. As a result, the relative magnitudes of  $^2J_{\text{Pt-P}_A}$  and  $^2J_{\text{Pt-P}_B}$  will reflect not only a difference in the type of ligands which are trans to the Pt-Pt bond but also their  $\sigma$ -donor ability.

### Conclusion

Studies presented in this paper of symmetrical and unsymmetrical dinuclear Pt(I) complexes containing phosphine ligands

(32) Jameson, C. J. In *Multinuclear NMR*; Mason, J., Ed.; Plenum Press: New York, 1987; p 107.

(33) Manojlovic-Muir, Lj.; Muir, K. W. *J. Organomet. Chem.* **1981**, *219*, 129.

clearly demonstrate that two-dimensional  $^{31}\text{P}$  correlated spectroscopy (COSY) available on high-field NMR spectrometers is a powerful technique for determining important coupling constant information. It has been shown for nine complexes, that the signs and magnitudes of the  $^2J_{\text{Pt-P}}$  coupling constant can be directly determined from the experimental two-dimensional spectrum by the appearance and position of cross correlations of the Pt-P satellite peaks. This method is especially valuable for systems of high complexity, where the internal multiplets of the Pt-P satellite peaks are poorly resolved or are obscured by the more intense central phosphorus resonance. In these cases, the two-bond Pt-P coupling constants cannot be determined from one-dimensional data. The determination of the  $^2J_{\text{Pt-P}}$  coupling constant is important for this class of compounds because it yields valuable information concerning the nature of the Pt-Pt bond and the effect of the ligands on this bond.

**Acknowledgment.** This project was supported by the Petroleum Research Fund and the National Science Foundation (Grant CHE-8416730). J.V.Z.K. gratefully acknowledges this support and the valuable assistance provided by Dr. Jerry Dallas and the Medical Systems Group at GE Instruments, Fremont, CA, in obtaining the COSY spectrum of **1**. The Department of Chemistry and Biochemistry at San Francisco State University acknowledges support received from the National Science Foundation (Grant DMB-8516065) and the National Institutes of Health (Grant RR-02684) for the purchase of the General Electric QE-300 and GN-300 NMR spectrometers.

**Supplementary Material Available:** The one- and two-dimensional  $^{31}\text{P}$  NMR spectra of complexes **3**, **4**, and **7-9** (6 pages). Ordering information is given on any current masthead page.

Contribution from the Department of Chemistry,  
Texas A&M University, College Station, Texas 77843-3255

## Theoretical Studies of Inorganic and Organometallic Reaction Mechanisms. 4. Oxidative Addition of Dihydrogen to $d^8$ Square-Planar Iridium Complexes with Trans Phosphines

Andrew L. Sargent and Michael B. Hall\*

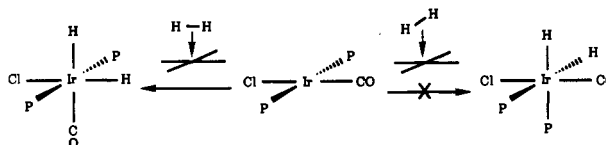
Received June 5, 1991

The oxidative addition of  $\text{H}_2$  to Vaska-type complexes,  $\text{trans-IrX}(\text{CO})(\text{PR}_3)_2$ , is investigated with ab initio quantum chemical calculations. The direction of addition in these complexes is controlled by how the ligands in the plane of addition react to a close encounter with concentrations of charge density around the metal center as the complex evolves from a four-coordinate to a six-coordinate species. Strong electron-donating ligands destabilize the five-coordinate transition state while electron-withdrawing ligands stabilize the transition state. When X is a weak electron donor ligand such as Cl,  $\text{H}_2$  adds in the Cl-Ir-CO plane. When X = H<sup>-</sup> or Ph<sup>-</sup>, however,  $\text{H}_2$  adds in the  $\text{PR}_3\text{-Ir-PR}_3$  plane; the destabilizing influence of these strong electron-donating ligands on the transition state outweigh those of the  $\text{PR}_3$  ligands. The electronic contribution to the relative stabilities of the six-coordinate final products can be predicted based on the relative orientations of the strongest trans-influence ligands. The isomers in which these ligands are facial are lower in energy than those in which they are meridional.

### Introduction

The activation of  $\text{H}_2$  through an oxidative-addition reaction with a transition-metal complex is a fundamental step in several important catalytic cycles.<sup>1</sup> In catalytic hydrogenation and hydroformylation, for example,  $\text{H}_2$  is activated by oxidative addition to a transition-metal center.<sup>2</sup> The oxidative addition of  $\text{H}_2$  to  $\text{trans-IrCl}(\text{CO})(\text{PPh}_3)_2$ , Vaska's complex, has been extensively studied,<sup>3</sup> and the generally accepted mechanism of the reaction involves the concerted addition of  $\text{H}_2$  to form pseudooctahedral products with a cis orientation of the hydride ligands.

Two isomeric products are possible in this reaction, and their formation can be viewed as the result of the concerted addition in one of the two vertical L-M-L planes of the  $d^8$  square-planar transition-metal complex. For Vaska's complex, only one isomer is observed, as shown in eq 1, and despite the large quantity of



(1)

- (1) Cotton, F. A.; Wilkinson, G. *Advanced Inorganic Chemistry*, 5th ed.; Wiley: New York, 1988; p 1186.  
 (2) Parshall, G. W. *Homogenous Catalysis*; Wiley: New York, 1980.  
 (3) (a) Chock, P. B.; Halpern, J. *J. Am. Chem. Soc.* **1966**, *88*, 3511. (b) Halpern, J. *Acc. Chem. Res.* **1970**, *3*, 386. (c) Vaska, L. *Ibid.* **1968**, *1*, 335. (d) Ugo, R.; Pasini, A.; Fusi, A.; Cenini, S. *J. Am. Chem. Soc.* **1972**, *94*, 7364. (e) Collman, J. P. *Acc. Chem. Res.* **1968**, *1*, 136.

work that has been devoted to the reaction, the specific factors which determine this stereochemistry remain largely unknown.

The analysis of the factors, which control the direction of  $\text{H}_2$  addition to Vaska's complex, is complicated by their sheer number. These factors include the combined steric and electronic contri-